Eriodictyol protects skin cells from UVA irradiation-induced photodamage by inhibition of the MAPK signaling pathway

Muhammad Farrukh Nisar[1#†], Tiantian Liu[1#], Mei Wang[1], Shida Chen[1], Li Chang[1], Vega Widya Karisma[1], Wei Xu[2], Qingchun Diao[2], Mei Xue[2], Xueyong Tang[2], Chararеh Pourzand[3], Jing Yang[1*], Julia Li Zhong[1*]

[1]Bioengineering College & Three Gorges hospital, Chongqing University, Chongqing 400044, China.
[2]Department of Dermatology, Chongqing First People's Hospital and Chongqing Traditional Chinese Medicine Hospital, No. 40 Daomenkou St., District Yuzhong, Chongqing 400011, P.R. China.
[3]Medicines Development, Centre for Therapeutic Innovation &Medicines Design, Department of Pharmacy & Pharmacology, University of Bath, Bath BA2 7AY, United Kingdom.
[#]Equal contribution
*Correspondence:
JL Zhong: jlzhong@cqu.edu.cn, College of Bioengineering; or Jing Yang: Three Gorges Hospital, Chongqing University, Chongqing 400044, P. R. China. Tel.: +86-15802371097; fax: +86-23-65102507. E-mail address: jlzhong@cqu.edu.cn or liutiantian579@sina.cn

[†]Current Address: Department of Physiology and Biochemistry, Cholistan University of Veterinary and Animal Sciences (CUVAS), Bahawalpur, 63100, Pakistan.

Graphical Abstract

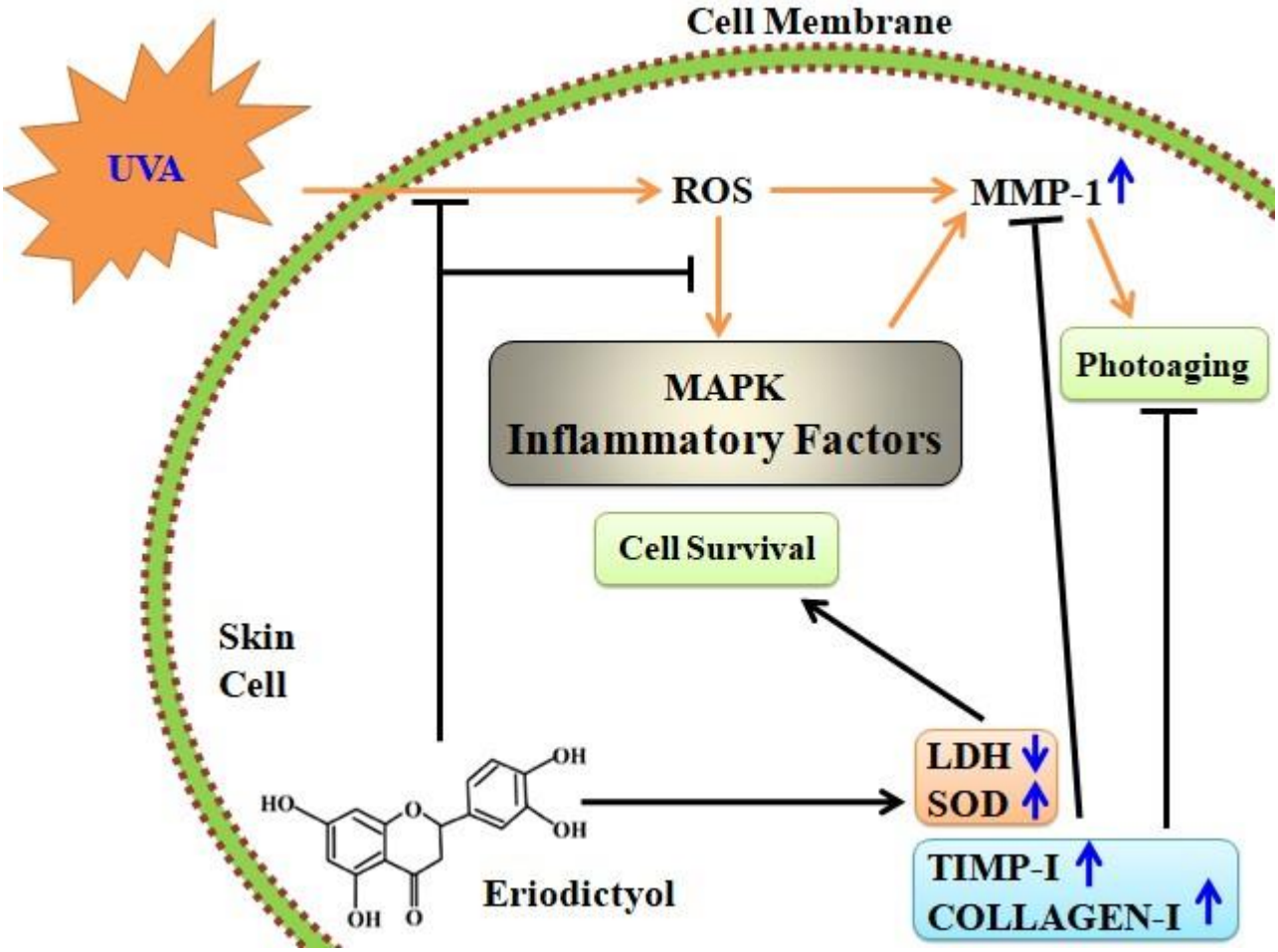

Abstract

Solar UVA irradiation-generated reactive oxygen species (ROS) induces the expression of matrix metalloproteinase 1 (MMP-1), leading to photoaging, however the molecular mechanism remains unclear. In the present study, we found that eriodictyol remarkably reduces UVA-mediated ROS generation and protects the skin cells from oxidative damage and the ensuing cell death. Moreover eriodictyol pretreatment significantly down-regulates the UVA-induced MMP-1 expression, and lowers the inflammatory responses within the skin cells. Pretreatment with eriodictyol upregulates the expression of tissue inhibitory metalloproteinase 1 (TIMP-1) and collagen-I (COL-1) at the transcriptional level in a dose-dependent manner. UVA-induced phosphorylation levels of c-Jun N-terminal kinase (JNK), extracellular signal-regulated kinase (ERK) and p38 leading to increased MMP-1 expression are significantly reduced in eriodictyol-treated skin cells. In addition, eriodictyol pretreatment significantly suppresses inflammatory cytokines and inhibits the activation of MAPK signalling cascades in skin cells. Taken together, our results demonstrate that eriodictyol has both potent anti-inflammatory and anti-photoaging effects.

Keywords: UVA, Eriodictyol, MMP-1, COL-1,TIMP-1, ROS, MAPK, Anti-photoaging.

1. Introduction

Sunlight is an important environmental factor which is divided into various electromagnetic radiations such as ultraviolet (UV) light spanning 100-400 nm of solar spectrum. UVA (320-400 nm) makes its way through the ozone layer to approach biosphere (Diffey, 2002, Nisar et al., 2015, Sklar et al., 2013). UVA has longer wavelengths and therefore has less energy than shorter UVB (280-320 nm) component of sunlight. Nevertheless, compared to UVB,UVA penetrates much deeper into the dermal and subcutaneous tissues of the skin (De Gruijl, 2002, York and Jacobe, 2010). Human skin is exposed to these UV radiations which are simultaneously detrimental and useful (Nisar et al., 2015, Tyrrell, 1996). It is reported that a low dose exposure to UVA light may provide not only beneficial (der Leun Van, 1994) but also therapeutic effects to pathological skin conditions (Reeve and Tyrrell, 2007), particularly in scleroderma, psoriasis and vitiligo (Krutmann et al., 2001, Stege et al., 1997). Chronic exposure of solar UVA radiation to human skin may aid the accumulation of excessive and persistent levels of ROS that imbalances the redox status of the cells and initiate pro-inflammatory factors (Kvam et al., 1999, Pourzand et al., 1999). Certain cellular built in mechanism provides protection and safeguard the cells and tissues against UVA-generated oxidative membrane damage (Ryter and Tyrrell, 2000). UVA mainly shows its effects in the skin by generating ROS that imbalance the redox homeostasis in the skin cells (Keyse and Tyrrell, 1987, Keyse and Tyrrell,

1989). The latter can be modified and protected by activation of natural built-in antioxidant enzymes such as nuclear factor erythroid 2-related factor 2(Nrf2)/heme oxygenase 1 (HO-1) pathway in human skin cells (Keyse and Tyrrell, 1987, Keyse and Tyrrell, 1989, Zhong et al., 2011, Zhong et al., 2010). Yang and colleagues used a natural cytoprotective antioxidant Acetyl-11-keto-β-Boswellic Acid(AKBA), that enhanced the protection in UVA exposed HaCaT cells and increased the cell proliferation by suppressing the ROS levels (Yang et al., 2017).

UVA-generated ROS is a serious threat to biomembranes (Tyrrell, 2012), and induce the expression of matrix metalloproteinases-1 (MMP-1) that deteriorates the organization of collagen and elastic fibers in the dermal extracellular matrix (ECM), resulting in a variety of skin conditions particularly photoaging and skin cancer (Ridley et al., 2009). Photoaging is generally described as a UV- driven premature aging of the skin compartments accompanied by increase in wrinkle formation, higher pigmentation, and leathery texture of the skin (Jenkins, 2002). Normally, the expression of MMPs and breakdown of collagens are under tight control and aided by the tissue inhibitors of the matrix metalloproteinases (TIMP-1 and -2) (Nagase and Woessner Jr, 1999). Many of the natural phytochemicals are reported to reduce the UVA-mediated cellular damages such as AKBA (Yang et al., 2017). Apigenin and luteolin can inhibit UVA-induced collagenolytic MMP-1 production by interfering with Ca^{2+}-dependent MAPKs and AP-1 signaling, therefore preventing the skin photoaging (Hwang et al., 2011). Hispidulin, sulforaphane, AKBA and neferine are potent anti-photoaging agents, providing cellular protection against UVA mediated cell damages mainly by scavenging the ROS, reducing the lipid peroxidation to restore cellular antioxidant levels along with inhibition of MMP-1 expression (Chaiprasongsuk et al., 2017, Khan et al., 2018, Yang et al., 2017).

Eriodictyol is a flavonoid present in many of citrus fruits and herbs (Zhong et al., 2016). It has diverse biological properties imparted mainly by its antioxidant and anti-inflammatory potentials (Mokdad-Bzeouich et al., 2016, Chobot et al., 2016, Lee et al., 2015). Recently, eriodictyol has been studied extensively and its cytoprotective capability is evidenced in a considerable number of reports (Xie et al., 2019). Its cytoprotective effects are mainly due to its role in controlling and regulating the mitochondrial physiology to check the apoptotic pathways. Nevertheless the effects of eriodictyol on the skin cells response under UV radiation stress are not yet to be fully elucidated.

In the present study, we evaluated the photoprotective effects of eriodictyol on skin cells (HaCaT keratinocytes and FEK4 fibroblasts) against the UVA radiation-induced oxidative damage by monitoring the expression of inflammatory factors and MMP-1 *in vitro*. We also examined how

eriodictyol affects expression levels of MMP-1, TIMP-1, COL-1, and phosphorylation states of MAPKs (JNK, ERK, p38) in UVA-irradiated skin cells.

2. Materials and Methods

2.1 Materials, reagents, antibodies

Materials, reagents, and antibodies include, fetal bovine serum (FBS, TBD21HY), RPMI 1640 medium (HyClone), high glucose Dulbecco's modified Eagle's medium (DMEM, Gibco), Eagle's minimum essential medium (EMEM, Invitrogen)dihydroethidium (DHE) (Jiancheng Institute of Biotechnology, Nanjing, China), Radioimmunoprecipitation assay buffer (RIPA buffer)(Beyotime, China), Phenylmethylsulfonyl fluoride (PMSF)(Beyotime, China), penicillin and streptomycin (North China Pharmaceutical CO, LTD, China), MMP-1 antibody (Santa Cruz Biotechnology Inc., USA), anti-β-actin antibody, the secondary antibodies against goat and rabbit IgG (Beijing Zhong Shan-Golden Bridge Biological Technology CO. LTD.), the secondary antibodies against mouse IgG (Beyotime, China); Eriodictyol (ER, ENZO Life Sciences), 3-[4,5-dimethyl-2-yl]-2,5-diphenyl-2H-tetrazolium bromide (MTT, Sigma, USA), Superoxide dismutase kit (SOD, Jiancheng Institute of Biotechnology, Nanjing, China) and kinase inhibitorsERK PD98059, JNK SP600125 and p38 SB203580 (Calbiochem, La Jolla, CA, USA).

2.2 Cell culture and treatments

Immortalized human skin keratinocyte cell line HaCaT cells were routinely cultured as described previously (Yang et al., 2017), and were kindly provided by Prof. Rex M. Tyrrell (University of Bath, UK). HaCaT cells were grown in high glucose DMEM containing 10%FBS, and protected by streptomycin and penicillin (1%), at 37°C and 5% CO_2. Cells were further passaged upon 80-85% confluency. The human primary skin fibroblasts FEK-4 were also kindly provided by Prof. Rex M. Tyrrell, University of Bath, UK.FEK-4 cells were maintained in EMEM supplemented with 10% FBS, 2 mM L-glutamine and 50 U/ml penicillin/streptomycin.

To determine the involvement of eriodictyol in modulation of MAPK (JNK, ERK, p38) pathway in MMP-1 expression, the skin cells were pretreated with 1 mM of the specific inhibitors (U0126, SP600125, and SB203580) for ERK, JNK, and p38, respectively, in serum-free medium for 1 hour before UVA irradiation.

2.3 UVA source, dosimetry and irradiation of cultured cells

UV light therapy system (Lifotronic) 365 nm (peak) spectrum lamp was used to irradiate cells (in PBS) following standard procedures, and non-irradiated cells were used as a background control

(control = 0 kJ/m2). A range of UVA doses (0, 25, 50, 75, 100, 150, 200, 250, 300, and 400 kJ/m^2) were given to the HaCaT and FEK-4 cells to optimize the irradiation condition using automated UV light therapy system (Lifotronic) 365nm (peak) spectrum lamp. We selected the comparable UVA dose (200 kJ/m^2 for HaCaT and 150 kJ/m^2 for FEK-4) that gave approximately 80% cell viability, which is consistent with the previous findings (Yang et al., 2017, Tian et al., 2011). The growth media of both cell lines (conditioned media) were kept aside and cells were washed twice with PBS and then irradiated in PBS. Following UVA irradiation, PBS was aspirated and cells were incubated in their respective conditioned medium.

2.4 MTT assay for cell viability

The HaCaT and FEK-4 cells were cultured in 96-well plates at a density of $8x10^3$/ per well for 12-24 h and then treated with eriodictyol at indicated concentrations (0, 5, 10, 20, 40 μM) for an additional 2 to 24 h prior to UVA irradiation. The cell viability was evaluated 24 h after UVA irradiation using the MTS (Promega) colorimetric assay and in a microplate reader (BioRad Benchmark Plusor BIO-RAD, 680) at 490 nm. The protective effect of eriodictyol under UVA stress on cell viability was calculated as the percent of viable cells compared with the vehicle control cells. The MTT assay was performed in triplicate from each of the three independent experiments.

2.5 Measurement of intracellular ROS

HaCaT and FEK-4 cells were seeded in 48-well plates. After 24h of incubation (60-70% confluence), the cells were treated with the eriodictyol for 12h in DMEM media containing 0.5% FBS. The generation of ROS was examined by the fluorescent staining with 10μM dihydroethidium (DHE). The intracellular ROS were visualized under a fluorescence microscope at the excitation and emission wavelengths of 480 and 530 nm, respectively. The relative fluorescence intensity was measured by using the Image-Pro Plus 7.0 software, and the statistical significance was analyzed using the OriginPro software program version 8.1.

2.6 Assay for cellular superoxide dismutase (SOD) and lactase dehydrogenase (LDH)

HaCaT and FEK-4 cells ($5x10^5$) were seeded in 6cm cell culture plates for 24h.The stock solution of eriodictyol was then prepared in 0.5% FBS-DMEM and added to the cultured cells at a final concentrations of 5, 10, 20, 40 μM. The eriodictyol treatment was carried out for 12 h, and then the cells were exposed to UVA at a dose of 150 kJ/m^2 in PBS. After irradiation, cells were incubated in their conditioned media for 4 h and then their proteins harvested using the RIPA buffer containing1% PMSF. The control cells were treated the same, except that were either not treated with eriodictyol and/or unirradiated with UVA. Based on WST-8 method, superoxide dismutase (SOD) assay was then performed using an SOD assay kit.LDH assay was used to determine the percentage of

extracellular LDH leakage. HaCaT and FEK-4 cells were seeded into 96-well plates (5000 cells/well) for 24h, followed by eriodictyol treatment (or not) for 12h at final concentrations of 5, 10, 20, 40 µM. Then the cells were sham- or UVA-irradiated for 4 h. The control cells were either untreated with eriodictyol, or sham-irradiated or their combinations. LDH release was measured using an LDH assay kit purchased from the Jiancheng Institute of Biotechnology (A020-2, Nanjing, China). The small amount of extracellular LDH is presenting as percent of total LDH and is expressed as the fold change relative to the sham (100%).

2.7 Enzyme-linked immunosorbent assay (ELISA) for MMP-1 expression

HaCaT cells were seeded ($1x10^5$) in 6-well plates. The cells were treated with eriodictyol and then UVA irradiated as explained in section *2.6*. The conditioned media were collected, concentrated, and quantified. The expression of MMP-1 was measured from three independent experiments (n=3) using a human MMP-1 ELISA Kit (Cat#CK-E93438R).

2.8 Gene expression analysis

To quantify gene expression levels, real-time qPCR experiments were carried out using the PromegaGoTaq® qPCR Master Mix (A6001) in a Light Cycler apparatus (C1000 Touch; Bio-Rad). In addition, expression of TIMP-1, Col-1, and the internal control GAPDH was also assessed by semi-quantitative real-time PCR. Specific primers were designed as shown in Table1.

Table 1: Primer sequences for PCR analysis.

Sr. No.	Name	5'-3'	Primer sequence
1	COX-2	F	ATGCTGACTATGGCTACAAAAGC
		R	TCGGGCAATCA TCAGGCAC
2	NFκB	F	AACAGAGAGGATTTCGTTTCCG
		R	TTTGACCTGAGGGTAAGACTTCT
3	IL-1β	F	TGAGCTCGCCAGTGAAATGA
		R	AACACGCAGGACAGGTACAG
4	IL-6	F	CTCAATATTAGAGTCTCAACCCCCA
		R	GAGAAGGCAACTGGACCGAA
5	TNF-α	F	CTGGGCAGGTCTACTTTGGG
		R	CTGGAGGCCCCAGTTTGAAT
6	TGF-β	F	GGGCTACCATGCCAACTTCT
		R	GACACAGAGATCCGCAGTCC
7	COL-1	F	CTGGAAGAGTGGAGAGTACTG
		R	TGCTGATGTACCAGTTCTTCTG
8	TIMP-1	F	ACTTCCACAGGTCCCACAAC
		R	GCATTCCTCACAGCCAACAG
9	GAPDH	F	GAAGATGGTGATGGGATTTC
		R	GAAGGTGAAGGTCGGAGTC
10	β-Actin	F	ACTCCTATGTGGGTGACGAGG

		R	CACACGCAGCTCATTGTAGAAG

2.9 Western blotting and Zymography

Whole-cell lysates were separated by sodium dodecyl sulfate-polyacrylamide gel electrophoresis (SDS-PAGE) with 12% gels and were transferred to PVDF membranes. Membranes were incubated with primary antibodies overnight. Primary antibodies include anti-β-Actin (Santa, sc-130065) and anti-MMP1 (Santa, sc-21731).The primary antibodies were detected by peroxidase-conjugated anti-mouse IgG or anti-rabbit IgG antibodies. Signals were examined using SuperSignal West Pico Substrate (Thermo, USA).MMP-1 secreted into the conditioned medium by the cells was also assayed using 0.05% gelatin zymography as described previously(Zhou et al., 2005).

2.10 Statistical analysis

All experiments were performed three times in duplicate. The data obtained in each experiment are presented as the mean±standard deviation (SD). The statistical significance was set by Student's t-test and p-values of < 0.05 were taken as significant. The significant difference was determined by one-way ANOVA. Statistical analyses were carried out by parametric and non-parametric ANOVA using OriginPro software program version 8.1.

3. Results

3.1 Effect of Eriodictyol on ROS generation in skin cells

The fluorescent intensity of DCFH-DA was used to calculate the intracellular ROS generation in HaCaT and FEK-4 fibroblasts cells (Figure 1). UVA irradiation doses of 200 kJ/m^2 (HaCaT cells) and 150 kJ/m^2 (FEK4 cells) induce a significant increase in ROS levels in both HaCaT (2.91+0.079-fold) and FEK-4 (4.887±0.21-fold) cells compared to the unirradiated and eriodictyol relative untreated) untreated controls. In both cell lines, pre-treatment with *2.5–40 μM* eriodictyol significantly decreased the efflux of intracellular ROS (Figures 1A-B). Pre-treatment of HaCaT cells with 40 μM eriodictyol significantly reduced the generation of ROS (1.15±0.084) compared to the UVA-irradiated group (2.91+0.079) (Figure 1A). Pre-treatment of FEK-4 cells with 20 μM eriodictyol significantly reduced the generation of ROS (1.48±0.217) compared to the UVA-irradiated group (4.88+0.21) (Figure 1B). These results indicate that eriodictyol efficiently blocks the generation of intracellular ROS.

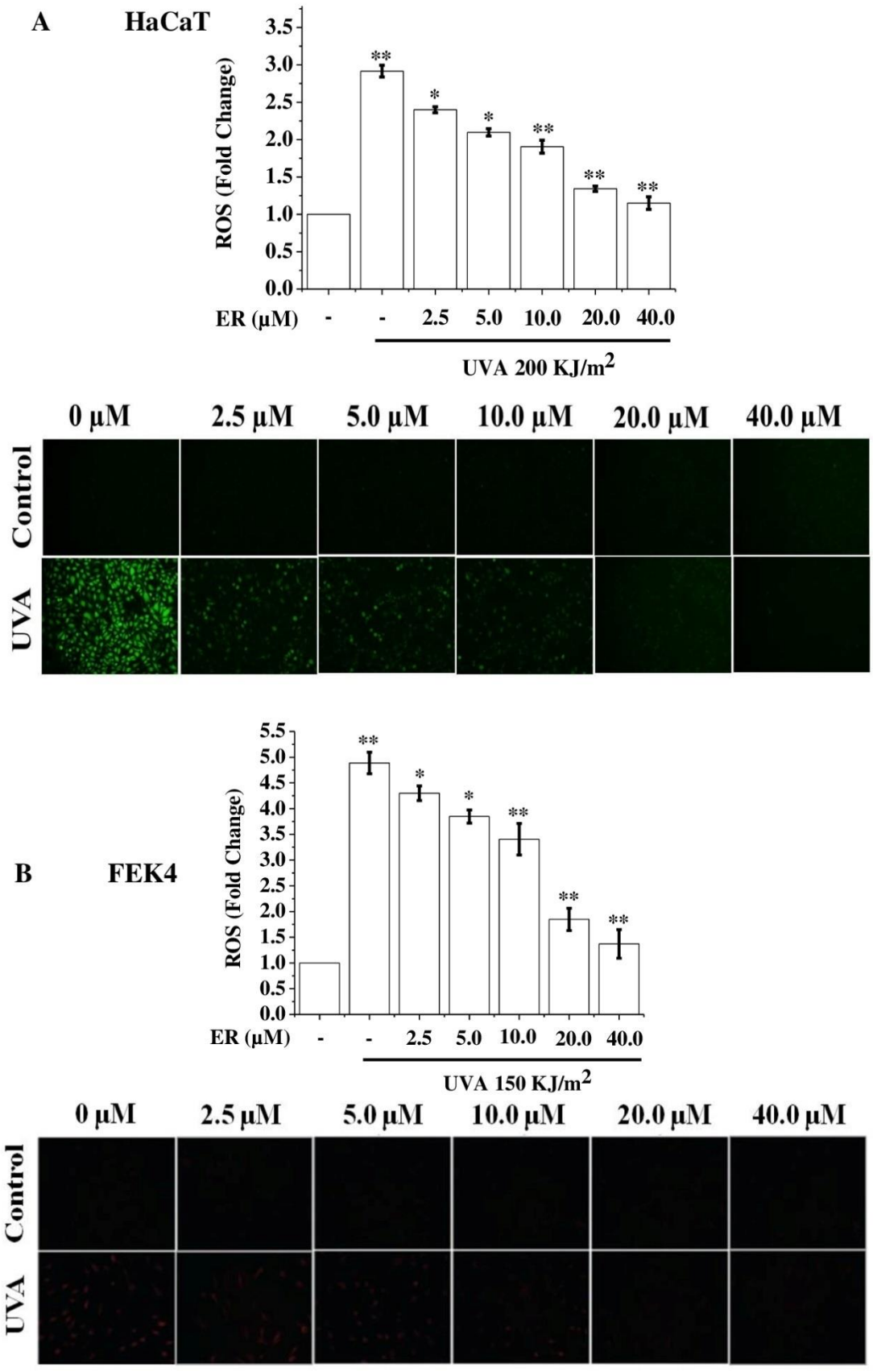
A
HaCaT
ROS (Fold Change)
3.5
3.0
2.5
2.0
1.5
1.0
0.5
0.0
**
*
*
**
**
**
ER (μM) - - 2.5 5.0 10.0 20.0 40.0
UVA 200 KJ/m2
0 μM
2.5 μM
5.0 μM
10.0 μM
20.0 μM
40.0 μM
Control
UVA
B
FEK4
ROS (Fold Change)
5.5
5.0
4.5
4.0
3.5
3.0
2.5
2.0
1.5
1.0
0.5
0.0
**
*
*
**
**
**
ER (μM) - - 2.5 5.0 10.0 20.0 40.0
UVA 150 KJ/m2
0 μM
2.5 μM
5.0 μM
10.0 μM
20.0 μM
40.0 μM
Control
UVA

Figure 1: Effect of eriodictyol (ER) on attenuation of ROS generation in UVA-irradiated human skin HaCaT and FEK4 fibroblasts. (A) The HaCaT cells were exposed to UVA (200 kJ/m^2) and immediately DCFH-DA staining was performed. Compared with the control, UVA increased the ROS while ER pre-treatment decreased the UVA-induced ROS generation in a concentration-dependent manner in HaCaT cells. (B) The FEK4 fibroblast cells were exposed to UVA (150 kJ/m^2) and immediately DCFH-DA staining was performed. The UVA exposure increased the ROS while ER pre-treatment decreased the UVA-induced ROS generation in a concentration-dependent manner in FEK4 cells. Values are expressed as a fold change relative to sham-treated control (which was set to 1). Data is expressed as mean±SD of three independent experiments in duplicates.

The HaCaT (A) and FEK4 fibroblast (B) cells were exposed to UVA (200 kJ/m^2 &150 kJ/m^2 respectively) and immediately DCFH-DA staining was performed. Compared with the control, UVA increased the ROS while ER pre-treatment decreased the UVA-induced ROS generation in a concentration-dependent manner. Values are expressed as a fold change relative to sham-treated control (which was set to 1). Data is expressed as mean±SD of three independent experiments in duplicates.

Many of the environmental as well as endogenous stresses in skin cells contribute to skin cancer, premature ageing or photoageing and chronic inflammatory disorders. UVA radiation is mainly involved in mediating indirect effects through the generation of ROS, causing inflammatory responses in the skin cells and hindering the antioxidant system resulting in imbalance in cellular redox status. qRT-PCR was used to evaluate whether eriodictyol can modulate the expression of various UVA-induced inflammatory factors in both skin cell types. As seen in Figure 2, UVA irradiation upregulated the expression of interleukins (IL-1β and IL-6), TGFβ, TNFα, COX-2 and NFκB in both HaCaT keratinocytes and FEK-4 fibroblasts. More specifically, UVA increased the expression of IL-1β about 1.8-fold and 1.2-fold in HaCaT and FEK-4 cells, respectively. When the cells were pre-treated with eriodictyol (20.0 μM), the expression of IL-1β was significantly ($p<0.01$) reduced to almost 50% value (1-fold) of the UVA-irradiated cells in both HaCaT and FEK-4 cells (Figure 2). In the case of UVA-mediated IL-6 expression, HaCaT keratinocytes (2.5-fold, $p<0.01$) showed almost 50% (half) of the expression of IL-6 observed in FEK-4 fibroblasts (5.0-fold, $p<0.05$), while compared to UVA treated alone, pre-treatment of eriodictyol down-regulated to 1.0-fold in HaCaT ($p<0.05$) and almost to 4.5-fold in FEK-4 cells ($p<0.01$)(Figure 2xxx).need labelABCD

UVA boosted the expression of TNFα in HaCaT keratinocytes and FEK-4 fibroblasts to 1.8- and 3.2-fold of their control values, respectively ($p<0.01$). In contrast pre-treatment of cells with eriodictyol (20 μM, you also have the 40μM in F1), reduced the UVA-mediated expression of TNFα to 1.8-and 3.2-fold of the UVA-irradiated values in HaCaT and FEK4 cells, respectively ($p<0.05$) (Figure 2).

Compared to their respective untreated control cells, HaCaT cells were more responsive to UVA and showed a greater increase in TGFβ expression (3.25-fold, $p<0.01$) than FEK-4 fibroblasts (1.5-fold, $p<0.05$). In eriodictyol pre-treated group of skin cells, HaCaT cells showed a marked and highly significant decline in expression of TGFβ (2.1-fold, $p<0.01$), FEK-4 fibroblasts showed much lower but still significant decline in TGFβ expression (0.75-fold, $p<0.05$) when compared to their corresponding UVA-treated cells (Figure 2).

UVA also modulated the expression of COX-2 in both cell types (Figure 2). In HaCaT cells, UVA increased the COX-2 expression up to 1.8-fold of control cells ($p<0.01$), while in FEK-4 cells, it rose to 9.1-fold of the control value ($p<0.01$). In HaCaT Cells, Eriodictyol pre-treatment (20 μM) significantly reduced the expression of COX-2 by0.7-fold of the UVA-irradiated controls, ($p<0.05$), while in FEK-4 cells, the level of expression was reduced even more to about 2.0-fold ($p<0.01$) of the corresponding UVA-irradiated FEK4 control cells. Finally, the modulation in the expression of NFκB was also examined in both skin cell type. The results revealed that in HaCaT cells, UVA can strongly ($p<0.01$) upregulated the expression of NFκB up to 7.2-fold, when compared to unirradiated cells. In comparison, in FEK4 cells the NFκB's expression was upregulated only up to3.6-fold, when compared to the unirradiated cells (Figure 2). Consistently, pre-treatment with eriodictyol (20 μM) ($p<0.01$) significantly reduced the activation of NFκB in HaCaT to about 4.9-fold of the UVA-irradiated cells alone when compared to the upregulation observed in FEK-4 fibroblast cells of about 1.1-fold of the UVA-irradiated cells alone.

3.3 Effect of UVA and Eriodictyol on skin cell viability

We used the MTS assay to evaluate the effect of UVA radiation, eriodictyol and combined effects (eriodictyol+UVA) on cell viability in human skin cells. Previously, our laboratory reported that a UVA dose of 200 kJ/m^2 could yield 78% of viable HaCaT cells (Yang et al., 2017). In the present study, we applied the same dose of 200 kJ/m^2 with a new UVA lamp, which also yielded a similar 75.9% viable HaCaT cells. For FEK-4 fibroblasts, a comparable UVA dose (150kJ/m^2) was selected in accordance to one of our previous studies (Unpublished data), yielding 75.4% viable FEK4 cells. We therefore applied the equil toxic doses of UVA on HaCaT (200 kJ/m^2) and FEK-4 (150 kJ/m^2) cells yielding 75.9% and 75.4% cell viability, respectively. Upon exposure to various doses of UVA, both cell lines showed a gradual increase in cell viability loss with increasing doses of UVA (Figure 3A). UVA radiation reduced the metabolic activity in both cell types in a dose-dependent manner, leading to cell death (Figure 3). The survival rate of HaCaT and FEK-4 cells was increased in a dose-dependent manner after cells were pre-treated with different concentrations of eriodictyol, compared

to controls (Figure 3B). High concentrations (40 μM) of eriodictyol pre-treatment had some cytotoxic effects on FEK-4 cells, as that the percentage cell viability was slightly decreased to 86.49%±8.11 (Figure 3B).

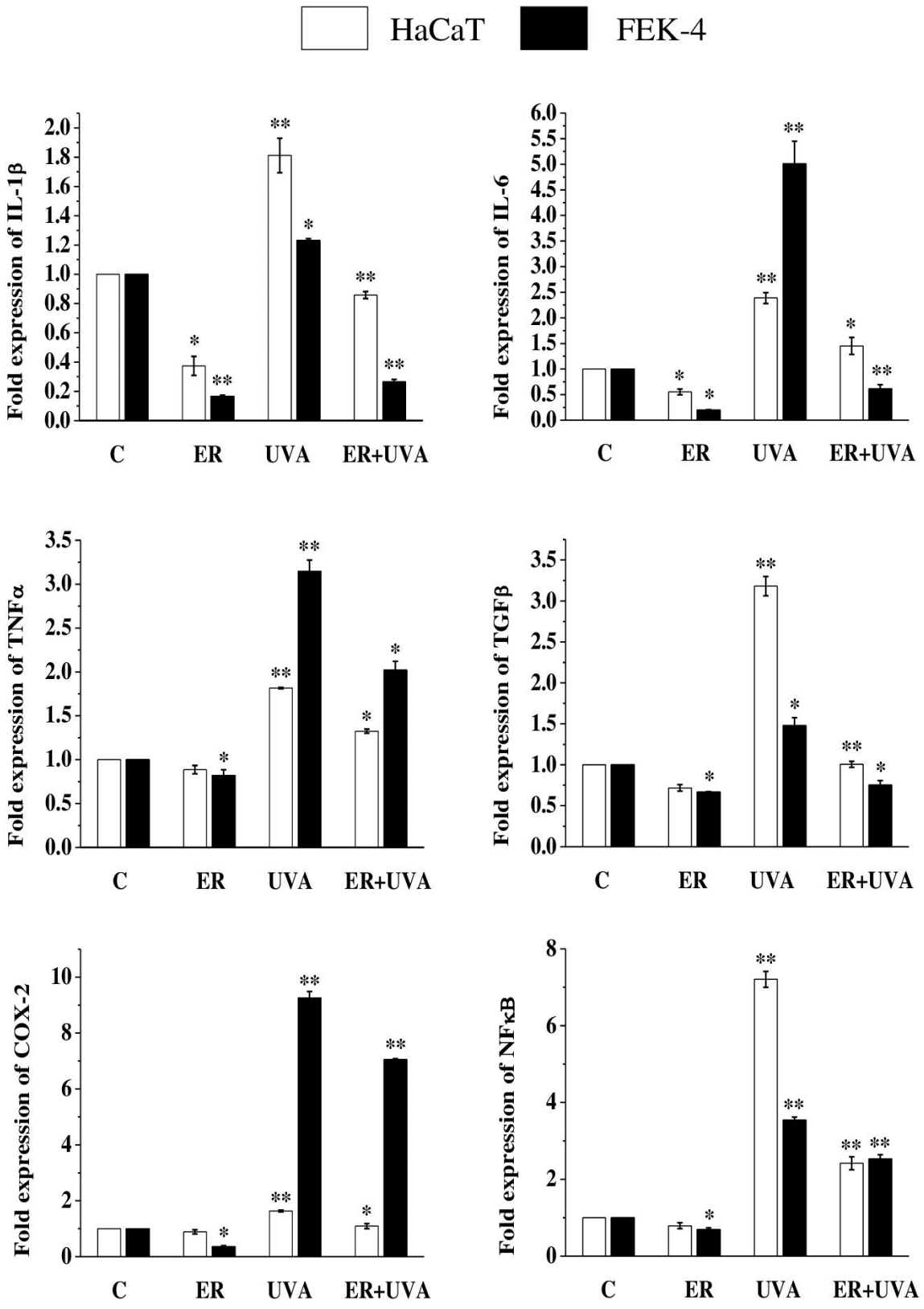
HaCaT
FEK-4
Fold expression of IL-1β
Fold expression of IL-6
Fold expression of TNFα
Fold expression of TGFβ
Fold expression of COX-2
Fold expression of NFκB
C
ER
UVA
ER+UVA

Figure 2: Eriodictyol (ER) modulates UVA-induced inflammatory response in HaCaT and FEK-4 cells. ER posed a strong down-regulatory effect on UVA-mediated inflammatory factors namely IL-1β, IL-6, TNFα, TGFβ, COX-2 and NFκB. Pre-treatment of HaCaT and FEK-4 cells was performed with 20 μM ER for 12 h, and the mRNA was extracted at 3 h post-UVA irradiation time points. Comparable UVA irradiations significantly increased the expression of these inflammatory factors, but pre-treatment with ER significantly suppressed UVA-mediated expression of inflammatory factors. Data are presented as mean±SD (n=3), *$p<0.05$, **$p<0.01$.

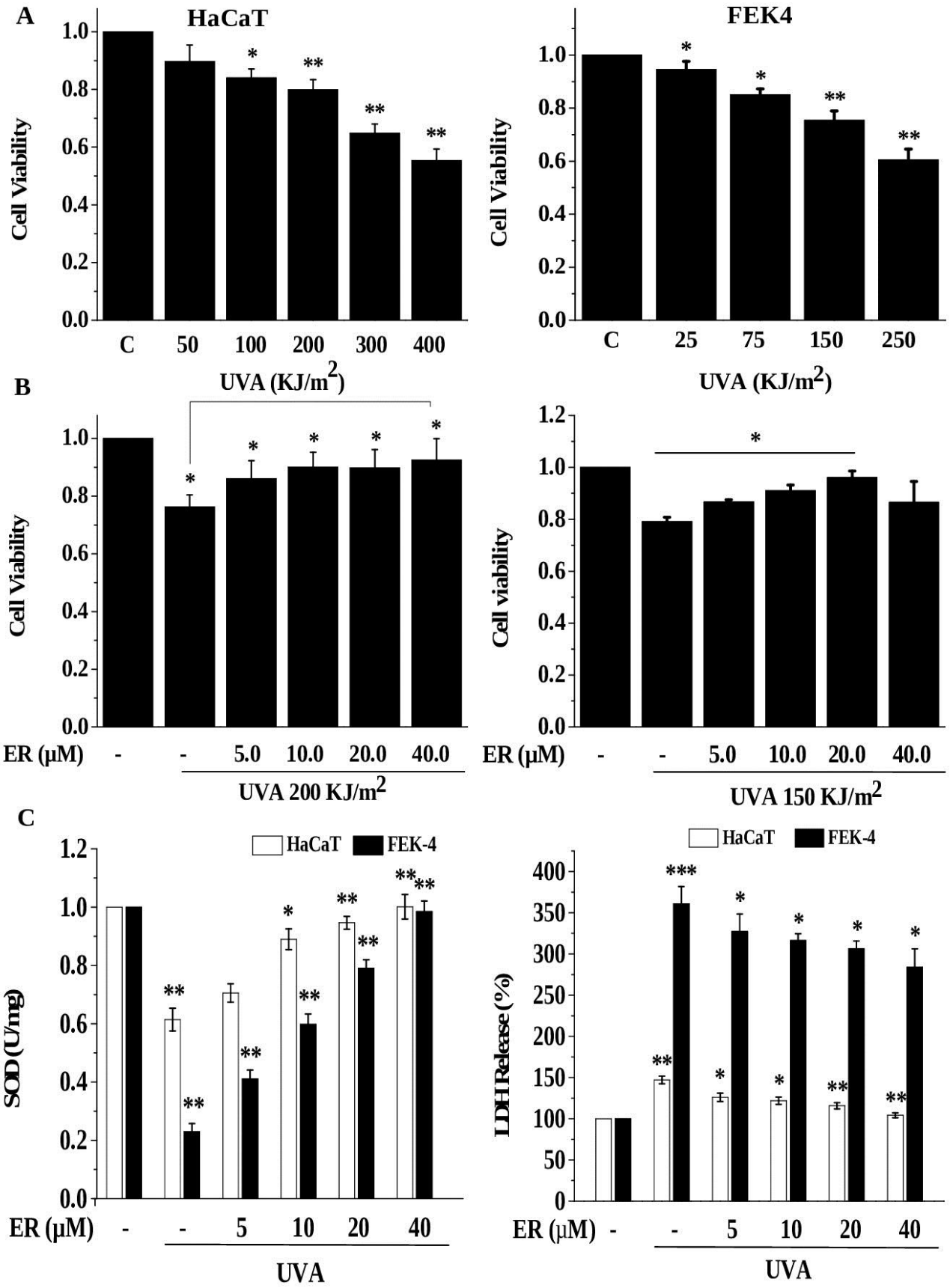
A
HaCaT
FEK4
Cell Viability
C
50
100
200
300
400
25
75
150
250
UVA (KJ/m2)
B
ER (μM)
5.0
10.0
20.0
40.0
UVA 200 KJ/m2
UVA 150 KJ/m2
C
HaCaT
FEK-4
SOD (U/mg)
LDH Release (%)
5
10
20
40
UVA

Figure 3: The cell viability and superoxide dismutase (SOD) and LDH release in HaCaT and FEK-4 cells. (A) The effect of a range of UVA doses on cell viability 24 h post UVA irradiation in HaCaT and FEK4 fibroblast cells. Increasing UVA doses significantly decreased cell viability after 24 h post irradiation in both cell lines, and 200 kJ/m^2 or 150 kJ/m^2 UVA dose was selected based on optimal cell survival (≈80%) for HaCaT and FEK-4 respectively, in follow-up experiments. **(B)** HaCaT and FEK-4 cells were pre-treated with eriodictyol (ER) for 12 h, which rescued cell viability loss in UVA-exposed cells, and increasing concentration of ER improved cell loss caused by UVA irradiation. All experiments used the same UVA dose, unless otherwise stated. Pre-treatment of HaCaT and FEK-4 cells with 20 μM of ER was set as optimal concentration. **(C)** SOD (left) was assayed 3 h following UVA irradiation, and eriodictyol significantly recovered UVA-mediated SOD depletion in both HaCaT and FEK-4 cells. (Right) Eriodictyol positively the UVA-induced LDH leakage in both HeCaT and FEK-4 cell lines exposed to UVA at 200 and 150 kJ/m^2, respectively. The numerical values are expressed as a relative percentage (%) to sham control, which was set to 1 (=100%). Both SOD activity and LDH leakage levels are presented as the mean±SD from three independent experiments in duplicates. *p<0.05, **p <0.01.

3.4 Effect of Eriodictyol on Superoxide dismutase (SOD) and LDH release in skin cells

When HaCaT keratinocytes were exposed to UVA radiation (200 kJ/m^2), the SOD activity was significantly decreased to 61.4% when compared to unirradiated control cells (set arbitrary as 100%). However with pre-treatment of cells with 40 μM eriodictyol recover the decrease to 95% of the control SOD level almost fully prevented the decrease in SOD activity in HaCaT cells following irradiation with the same dose of UVA-irradiated cell alone (Figure 3C). Similarly, in FEK-4 fibroblasts, UVA irradiation (150 kJ/m^2) alone reduced the SOD activity to 23.07% of the control but pre-treatment with different concentrations of eriodictyol rescued the SOD levels in a dose dependent manner. Interestingly, 40 μM eriodictyol pre-treatment increased the release of SOD in FEK-4 cells up to 98% of the control, when compared to UVA-treated cells alone (23%)(Figure 3C).

LDH is quite a stable enzyme present in cytosol, and it released during the cell rupture following UVA irradiation. The LDH leakage was quantified just after UVA exposure to find the cytoprotective effects of eriodictyol on the skin cells (Figure 3D). UVA irradiation significantly damaged the cells to release the LDH from HaCaT (147.075±4.6) and FEK-4 fibroblast cells (360.91±20.91) 4 h after UV exposure compared to the respective controls. While, pre-treatment with various indicated concentrations of eriodictyol suppressed the massive release of LDH from both the HaCaT and FEK-4 fibroblast cells in a concentration-dependent manner (Figure 3D). Taken together, eriodictyol strongly attenuated the UVA-driven membrane leakage and hence protected both skin cell types.

3.5*Eriodictyol inhibits MMP-1expression in HaCaT and FEK-4 fibroblast cells*

To evaluate the effects of UVA irradiation on the production of MMP-1, HaCaT keratinocytes and FEK-4 fibroblasts were exposed to UVA (200 & 150 kJ/m^2, respectively) alone or to

eriodictyol+UVA. Next, the MMP-1 protein expressions were measured by three assays of ELISA, Western blotting and Zymography (Figure 4). Comparing to the non-irradiated control cells, the ELISA results showed an increased production of MMP-1 in HaCaT keratinocytes (2.5-fold, **$p<0.01$) and FEK-4 fibroblasts (8.5-fold, **$p<0.01$) given the UVA (150 KJ/m^2) irradiation only (Figure 4A). The pre-treatment with various concentrations of eriodictyol down- regulated the production of MMP-1 in both the skin cell lines in a concentration dependent manner at 24 h post-UVA irradiation time point (Figure 4A). Moreover, Western blot assay also confirmed the significant down regulatory activity of pre-treatment with eriodictyol (20 μM) to UVA irradiated HaCaT and FEK-4 fibroblast cells (Figure 4B). Thus eriodictyol pre-treatment reduced UVA induced expression of MMP-1 in HaCaT and FEK-4 fibroblast cells. The Zymograms showed a similar pattern to the expression of MMP-1, which initially increased following UVA irradiation in both skin cells, but the eriodictyol treatment prior to UVA radiation prevented the down-regulation of MMP-1 expression, when compared to UVA-irradiated cells alone controls (Figure 4C). The MMP-1 activity was quantified using ImageJ software that measures the density of the bands appearing due to the digestion of the gel.

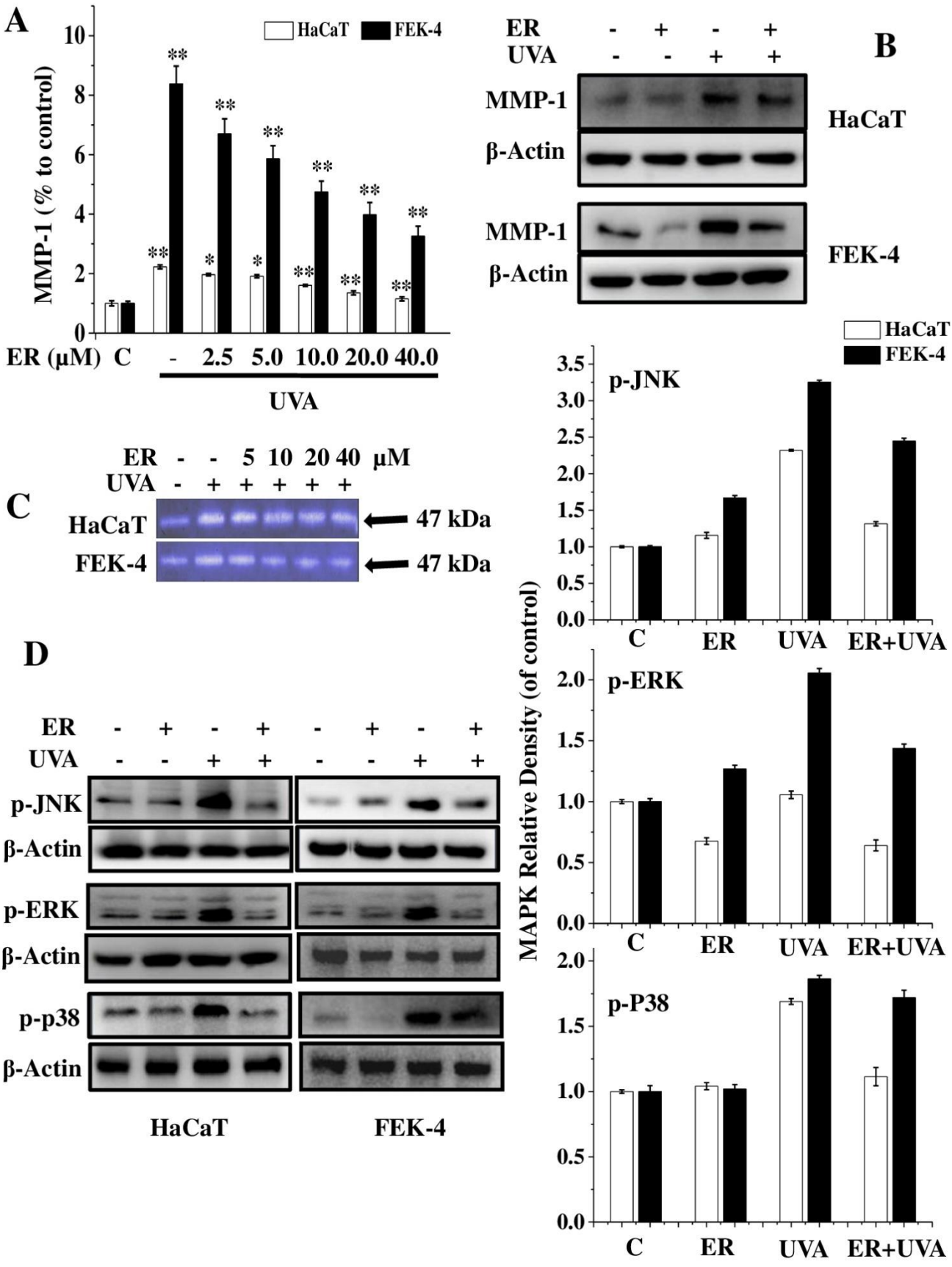
A
HaCaT
FEK-4
MMP-1 (% to control)
ER (μM) C - 2.5 5.0 10.0 20.0 40.0
UVA
B
ER - + - +
UVA - - + +
MMP-1
β-Actin
HaCaT
FEK-4
C
ER - - 5 10 20 40 μM
UVA - + + + + +
HaCaT
FEK-4
47 kDa
D
p-JNK
p-ERK
p-p38
β-Actin
HaCaT
FEK-4
MAPK Relative Density (of control)
C ER UVA ER+UVA

Figure 4: Effects of eriodictyol on the expression and secretion of UVA-induced MMP-1 in human skin HaCaT and FEK-4 fibroblast cells. Both cell types were pre-treated with 20 μM eriodictyol for 12 h. (A) The cell supernatants were collected, concentrated, the proteins concentrations were quantified by BCA method and MMP-1 expression in both cell lines was evaluated by ELISA. Western blot analyses showed modulation of MMP-1 (B) in both cell lines after 24 h treatment, respectively. (C) The Zymograms showing the digestion of the collagen gels which are the expression level of the MMP-1. (=100%). (D) Regulation of MAPKs (p-JNK, p-ERK, p-p38) activation by eriodictyol in human skin cells. The numerical values were obtained by densitometric measurements and expressed as a relative percentage (%) to their respective non-treated control set as 100%. MMP1 expression was presented as the mean±SD obtained from three separate experiments in duplicates; *p <0.05, **p <0.01.

3.6 Eriodictyol inhibits ERK, JNK, and p38 MAPK phosphorylation

Excessive efflux of ROS drives the activation of MAPK signalling cascade in HaCaT and FEK-4 cells following UVA exposure (Figure 4D). The activation of MAPK pathway activates the phosphorylation of its downstream transcription factors that ultimately triggers the expression of MMP-1 in HaCaT and FEK-4 cells. Eriodictyol is thought to check the expression of MMP-1, hence the effect of eriodictyol on inhibiting the phosphorylation of MAPK subfamilies JNK, ERK and p38 was determined (Figure 4D). Following the comparable UVA dose exposures, the phosphorylation of JNK, ERK and p38 was increased compared to their respective controls, while pre-treatment of skin cells with eriodictyol (20 μM) significantly ($p<0.01$) reduced the phosphorylation of MAPKs.

3.7 The effects of eriodictyol on TIMP-1 and COL-1 expression in UVA irradiated skin cells

The semi-quantitative RT-PCR was also employed to assess the effects of eriodictyol on UVA-irradiated HaCaT keratinocytes and FEK-4 fibroblasts and the expression of tissue inhibitory metalloproteinase 1 (TIMP-1) and collagen 1 (COL-1) (Figure 5). First, MMP-1's aid in inducing the collagen degradation following UVA exposures was confirmed. The expression of TIMP-1and COL-1were also detected in UVA-irradiated HaCaT keratinocytes and FEK-4 fibroblasts (Figure 5A, B). If the are the same loading, you need not set them as A and B, just merge. Results showed that TIMP-1 and COL-1 mRNA were significantly (**$p<0.01$) down- regulated following comparable UVA doses in both HaCaT and FEK-4 fibroblast cells. On the contrary, pre-treatment with various concentrations of eriodictyol (5, 10, 20 μM) followed by UVA irradiation, steadily ascends the expression of TIMP-1 (**$p<0.01$) and COL-1 (**$p<0.01$) in both cell lines with increasing eriodictyol concentrations (Figure 5A, B). It is clear from the results that eriodictyol could reduce the loss of TIMP-1 and COL-1expression in UVA-irradiated skin cells.

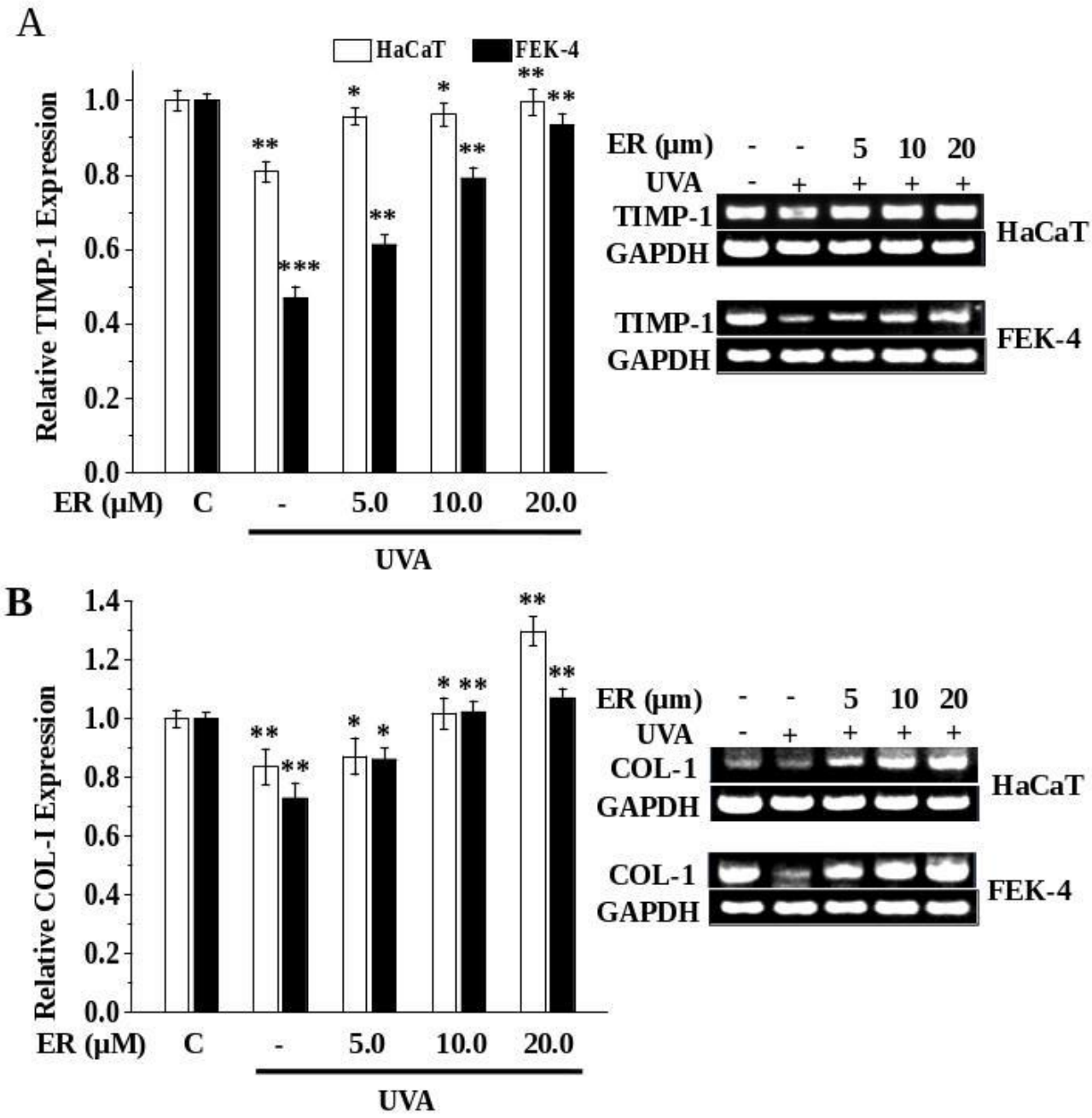
A
HaCaT
FEK-4
Relative TIMP-1 Expression
1.0
0.8
0.6
0.4
0.2
0.0
ER (μM) C - 5.0 10.0 20.0
UVA
ER (μm) - - 5 10 20
UVA - + + + +
TIMP-1
GAPDH
HaCaT
TIMP-1
GAPDH
FEK-4
B
Relative COL-I Expression
1.4
1.2
1.0
0.8
0.6
0.4
0.2
0.0
ER (μM) C - 5.0 10.0 20.0
UVA
ER (μm) - - 5 10 20
UVA - + + + +
COL-1
GAPDH
HaCaT
COL-1
GAPDH
FEK-4

Figure 5: The effect of UVA and eriodictyol on the expression of TIMP-1 and COL-1 in human skin HaCaT and FEK-4 cells. HaCaT and FEK-4 cells in control group, ？？UVA- treated and eriodictyol treated cells followed (or not) by UVA irradiation （combined UVA+/− eriodictyol treatment）were subjected to semi-quantitative RT-PCR,24 h after treatments. Relative expression level of (A) TIMP-1 and (B) COL-1 mRNA, in both groups was evaluated in three independent experiments. Quantitative data were presented relative to the untreated control group;*p <0.05, **p <0.01.

4. Discussion

Human skin not only defined the three dimensional structure of the body but also shields from various external harmful factors including UVR (Li et al., 2016, Nisar et al., 2015, Tyrrell, 2012). Chronic and repeated exposures to UVR cause various skin ailments particularly the sunburn, photoaging, photodermatosis and even skin cancer (Tyrrell, 2012). Low energy UVA penetrates deep into the skin (dermis, subcutaneous) to generate heavy burden of ROS (Tyrrell, 2012, Reeve and Tyrrell, 2007, Sklar et al., 2013, De Gruijl, 2002), and repeated UVA exposures accumulate massive and persistent ROS that imbalance of the redox status in skin cells. Moreover, UVA radiation releases free heme from microsomal protein bodies, degrades ferritin to raise labile iron, which may initiate proinflammatory factors and severe skin diseases (Kvam et al., 1999, Pourzand et al., 1999). ROS seriously damage biomembranes, biomolecules, induce the expression of matrix metalloproteinases (MMPs), and hence damage irreversibly the skin culminating into photo-aged skin (Fisher et al., 2002).

Many of the phytochemicals have extensively been reported to provide protection against UVA mediated skin damages and photoaging. Recently, we reported that AKBA (gum extract of *Boswellia serrata* L.) protects the skin cells from UVA-induced damage by modulating inflammatory mediators and ROS production, hence AKBA has been regarded as a potential candidate in the development of skin care products (Yang et al., 2017). Generally, the antioxidants provide cytoprotective effects *in vitro*. The eriodictyol being an antioxidant possesses diverse biological properties which contribute to its photoprotective effect against UV-induced cellular damage and apoptosis (Lee et al., 2011, Lee et al., 2007). Although eriodictyol has been recognized as a potential UVA and UVB filtering antioxidant (Rajan et al., 2018), it is still unclear how it promotes its anti-ageing effect against UV components of sunlight.

UVA irradiation reduced the cell viability in HaCaT keratinocytes and FEK-4 fibroblasts mainly due to the leakage of the cellular membranes (Tian et al., 2011, Zhong et al., 2014). Nevertheless, eriodictyol pre-treatment rescued UVA-induced cell death of both cell types in a dose-dependent manner by reducing both ROS generation and the related membrane damages. Similarly in various

other studies, eriodictyol has been shown to protect the cells against ROS-mediated cell injury and cell death (Lee et al., 2015, Lee, 2011, Xie et al., 2019). It is well known phenomenon that with increasing UVA doses, the cytoprotective mechanism related to Nrf2/HO-1 pathway gets suppressed, because of the dose-dependent increase in ROS which finally compromises the cellular redox balance and by induction of Kruppel-like factor 9 (Kfl9) may force the cells to die by apoptosis (Zucker et al., 2014). Eriodictyol is an antioxidant that protects the skin cells from heavy burden of oxidative stress (Rajan et al., 2018). The eriodictyol has potential shielding effects against UVA-induced damage in human skin cells notably HaCaT keratinocytes and FEK-4 fibroblasts, mainly due to its ability to enhance cellular proliferation and to decrease the intracellular ROS production by UVA and thereby reducing the level of UVA-induced cell death.

UVA exposure is known to initiate the synthesis of MMPs in the human skin (Fisher et al., 1997), and prolonged UVA exposure has been implicated in compromising the skin's natural defense system and thereby causing oxidative damage or inflammatory response mediated by COX-2 and NF-κB (Amano et al., 1998, Fisher et al., 2002, Wang et al., 2018). Various antioxidants or phytochemicals are reported to combat UVA-induced damages (Nisar et al., 2015, Yang et al., 2017). UVA-mediated ROS generation in skin cells can potentiate an indirect damage to irradiated cells (Valencia and Kochevar, 2008, Quyen et al., 2013) especially by targeting the DNA, lipids and proteins, and hence triggering an array of cellular signaling (Philips et al., 2004, Philips et al., 2003). The extracellular matrix (ECM), is of great importance in the tissues for cell to cell adhesions, communications, death signals, proliferation as well as skin integrity (Jackson et al., 2010).

Chronic skin inflammations may lead to tissue disintegration and loosening mainly by the involvement of over-expressed MMPs and ECM breakdown finally causing photoaging (Hong et al., 2009). Higher expression of UVA-mediated MMPs promoted breakdown of ECM, which disintegrates the skin collagen tissue and synthesis of ECM (Wlaschek et al., 1994). The up-regulation of MMP-1 and the breakdown of skin collagen tissue after UVA exposures were studied herein, and it was seen that eriodictyol potentially reduced the expression of UVA-mediated MMP-1, which might prevent the wrinkles formation or photoaging in the skin. The results of the present study strongly suggest that the down-regulation of MMP-1 and up-regulation of TIMP-1 andCOL-1 activity following UV-exposures in HaCaT and FEK-4 cells is possibly linked to the inhibition of ROS production by eriodictyol. Various other compounds have previously been reported to efficiently lower or reduce the UVA-mediated expression of MMP-1, reduce the UVA-generated ROS and LDH leakage, hence avoiding or slowing down the premature skin aging and delaying photoaging (Pallela et al., 2010).

The MAPK signalling cascade is activated in the cells upon UVA exposure, and actively transmits signals into the nucleus, where it plays key roles in activating downstream genes to regulate apoptosis or MMPs expression (Hwang et al., 2011). Consistent with previous studies using other phytochemicals (Hwang et al., 2011, Lee et al., 2011, Chaiprasongsuk et al., 2017), we show here that eriodictyol can down-regulate MMP-1 expression by reducing the UVA-induced phosphorylation of JNK, ERK, and p38 in the present study.

5. Conclusions

In conclusion, our study showed that eriodictyol has protective effects in both HaCaT and FEK-4 cells subjected to UVA irradiation, through enhancing cell proliferation, reducing the intracellular ROS generation and downregulating the expression of inflammatory factors and MMP-1, but upregulating the expression of Timp1 and Col1. Therefore, eriodictyol can be considered as a potential drug to confer photoprotection.

Author Contributions: MFN, TTL, MYW,WSDC, MJZ performed the experiments. MFN, MW, LC, XH, JY helped to arrange the data. CP, WX, LY and JLZ conceptualized this study. MFN, XYT, QCD, JY, CP and JLZ wrote this manuscript.

Funding: This work is financially supported by The National Science Foundation of China (No. 81704091, 81271776, 81573073). Series of Evidence Based Study on Hot Spring Wellness, Chongqing Municipal Commission of Culture and Tourism Development (To JL Zhong). The Fundamental Research Funds for the Central Universities. 2020CDJYGSG003. Key projects of Chongqing Municipal Science and Technology Commission (cstc2017jcyjbx0044). China Postdoctoral Science Foundation (Grant No. 2019M653348). Natural Science Foundation of Chongqing, China, (cstc2019jcyj-msxmX0757).

Acknowledgments: We acknowledge Prof. Joerg W. Bartsch for critical review and revision.

Conflicts of Interest: All the authors listed in the author section declare no conflict of interest for the submission and publication of this work. All authors agreed to submit this article to Journal of Photochemistry and Photobiology B: Biology.

Data Availability Statement: The data can be produced and presented upon demand.

References

AMANO, H., KUROSAWA, M. & MIYACHI, Y. 1998. Inhibition of substance-P-induced histamine release from rat peritoneal mast cells by 8-methoxypsoralen plus long-wave ultraviolet light irradiation: decreased intracellular calcium as a possible mechanism. *International archives of allergy and immunology,* 115**,** 55-60.

CHAIPRASONGSUK, A., LOHAKUL, J., SOONTRAPA, K., SAMPATTAVANICH, S., AKARASEREENONT, P. & PANICH, U. 2017. Activation of Nrf2 reduces UVA-mediated MMP-1 upregulation via

MAPK/AP-1 signaling cascades: the photoprotective effects of sulforaphane and hispidulin. *Journal of Pharmacology and Experimental Therapeutics,* 360**,** 388-398.

CHOBOT, V., HADACEK, F., BACHMANN, G., WECKWERTH, W. & KUBICOVA, L. 2016. Pro-and antioxidant activity of three selected flavan type flavonoids: catechin, eriodictyol and taxifolin. *International journal of molecular sciences,* 17**,** 1986.

DE GRUIJL, F. R. 2002. Photocarcinogenesis: UVA vs. UVB radiation. *Skin pharmacology and physiology,* 15**,** 316-320.

DER LEUN VAN, J. 1994. Estimate of the wavelength dependency of ultraviolet carcinogenesis in humans and its relevance to the risk assessment of a stratospheric ozone depletion. *Health physics,* 67**,** 319-325.

DIFFEY, B. L. 2002. What is light? *Photodermatology, photoimmunology & photomedicine,* 18**,** 68-74.

FISHER, G. J., KANG, S., VARANI, J., BATA-CSORGO, Z., WAN, Y., DATTA, S. & VOORHEES, J. J. 2002. Mechanisms of photoaging and chronological skin aging. *Archives of dermatology,* 138**,** 1462-1470.

FISHER, G. J., WANG, Z., DATTA, S. C., VARANI, J., KANG, S. & VOORHEES, J. J. 1997. Pathophysiology of premature skin aging induced by ultraviolet light. *New England Journal of Medicine,* 337**,** 1419-1429.

HONG, H., PARK, Y.-K., CHOI, M.-S., RYU, N.-H., SONG, D.-K., SUH, S.-I., NAM, K.-Y., PARK, G.-Y. & JANG, B.-C. 2009. Differential down-regulation of COX-2 and MMP-13 in human skin fibroblasts by glucosamine-hydrochloride. *Journal of dermatological science,* 56**,** 43-50.

HWANG, Y. P., OH, K. N., YUN, H. J. & JEONG, H. G. 2011. The flavonoids apigenin and luteolin suppress ultraviolet A-induced matrix metalloproteinase-1 expression via MAPKs and AP-1-dependent signaling in HaCaT cells. *Journal of dermatological science,* 61**,** 23-31.

JACKSON, B. C., NEBERT, D. W. & VASILIOU, V. 2010. Update of human and mouse matrix metalloproteinase families. *Human genomics,* 4**,** 194.

JENKINS, G. 2002. Molecular mechanisms of skin ageing. *Mechanisms of ageing and development,* 123**,** 801-810.

KEYSE, S. M. & TYRRELL, R. M. 1987. Both near ultraviolet radiation and the oxidizing agent hydrogen peroxide induce a 32-kDa stress protein in normal human skin fibroblasts. *Journal of Biological Chemistry,* 262**,** 14821-14825.

KEYSE, S. M. & TYRRELL, R. M. 1989. Heme oxygenase is the major 32-kDa stress protein induced in human skin fibroblasts by UVA radiation, hydrogen peroxide, and sodium arsenite. *Proceedings of the National Academy of Sciences,* 86**,** 99-103.

KHAN, A., BAI, H., SHU, M., CHEN, M., KHAN, A. & BAI, Z. 2018. Antioxidative and Anti-photoaging Activities of Neferine upon UVA Irradiation in Human Dermal Fibroblasts. *Bioscience Reports*, BSR20181414.

KRUTMANN, J., MORITA, A. & ELMETS, C. A. 2001. Mechanisms of photo (chemo) therapy. *Dermatological phototherapy and photodiagnostic methods.* Springer.

KVAM, E., NOEL, A., BASU-MODAK, S. & TYRRELL, R. M. 1999. Cyclooxygenase dependent release of heme from microsomal hemeproteins correlates with induction of heme oxygenase 1 transcription in human fibroblasts. *Free Radical Biology and Medicine,* 26**,** 511-517.

LEE, E.-R., KIM, J.-H., CHOI, H. Y., JEON, K. & CHO, S.-G. 2011. Cytoprotective effect of eriodictyol in UV-irradiated keratinocytes via phosphatase-dependent modulation of both the p38 MAPK and Akt signaling pathways. *Cellular Physiology and Biochemistry,* 27**,** 513-524.

LEE, E.-R., KIM, J.-H., KANG, Y.-J. & CHO, S.-G. 2007. The anti-apoptotic and anti-oxidant effect of eriodictyol on UV-induced apoptosis in keratinocytes. *Biological and Pharmaceutical Bulletin,* 30**,** 32-37.

LEE, J., NOH, A. L. S. M., ZHENG, T., KANG, J.-H. & YIM, M. 2015. Eriodicyol inhibits osteoclast differentiation and ovariectomy-induced bone loss in vivo. *Experimental cell research,* 339**,** 380-388.

LEE, J. K. 2011. Anti-inflammatory effects of eriodictyol in lipopolysaccharidestimulated raw 264.7 murine macrophages. *Archives of pharmacal research,* 34**,** 671-679.

LI, M., LIN, X.-F., LU, J., ZHOU, B.-R. & LUO, D. 2016. Hesperidin ameliorates UV radiation-induced skin damage by abrogation of oxidative stress and inflammatory in HaCaT cells. *Journal of Photochemistry and Photobiology B: Biology,* 165**,** 240-245.

MOKDAD-BZEOUICH, I., MUSTAPHA, N., SASSI, A., BEDOUI, A., GHOUL, M., GHEDIRA, K. & CHEKIR-GHEDIRA, L. 2016. Investigation of immunomodulatory and anti-inflammatory effects of eriodictyol through its cellular anti-oxidant activity. *Cell Stress and Chaperones,* 21**,** 773-781.

NAGASE, H. & WOESSNER JR, J. 1999. Matrix metalloproteinases J Biol Chem 274 (31): 21491–21494. *Find this article online*.

NISAR, M. F., PARSONS, K. S. G., BIAN, C. X. & ZHONG, J. L. 2015. UVA Irradiation Induced Heme Oxygenase-1: A Novel Phototherapy for Morphea. *Photochemistry and photobiology,* 91**,** 210-220.

PALLELA, R., NA-YOUNG, Y. & KIM, S.-K. 2010. Anti-photoaging and photoprotective compounds derived from marine organisms. *Marine drugs,* 8**,** 1189-1202.

PHILIPS, N., BURCHILL, D., O'DONOGHUE, D., KELLER, T. & GONZALEZ, S. 2004. Identification of benzene metabolites in dermal fibroblasts as nonphenolic: regulation of cell viability, apoptosis, lipid peroxidation and expression of matrix metalloproteinase 1 and elastin by benzene metabolites. *Skin pharmacology and physiology,* 17**,** 147-152.

PHILIPS, N., SMITH, J., KELLER, T. & GONZALEZ, S. 2003. Predominant effects of Polypodium leucotomos on membrane integrity, lipid peroxidation, and expression of elastin and matrixmetalloproteinase-1 in ultraviolet radiation exposed fibroblasts, and keratinocytes. *Journal of dermatological science,* 32**,** 1-9.

POURZAND, C., WATKIN, R. D., BROWN, J. E. & TYRRELL, R. M. 1999. Ultraviolet A radiation induces immediate release of iron in human primary skin fibroblasts: the role of ferritin. *Proceedings of the National Academy of Sciences,* 96**,** 6751-6756.

QUYEN, B. T., CHOI, H. K. & KANG, K. W. 2013. Pin1 is required for ultraviolet A-stimulated cyclooxygenase-2 induction in mouse epidermal cells. *Cancer Lett,* 335**,** 31-40.

RAJAN, V. K., TK, S. A. & MURALEEDHARAN, K. 2018. Data on the UV filtering and radical scavenging capacity of the bitter masking flavanone Eriodictyol. *Data in brief,* 20**,** 981-985.

REEVE, V. & TYRRELL, R. M. 2007. UVA and inducible protection. *Biophysical and Physiological Effects of Solar Radiation on Human Skin.* Cambridge: The Royal Society of Chemistry.

RIDLEY, A. J., WHITESIDE, J. R., MCMILLAN, T. J. & ALLINSON, S. L. 2009. Cellular and sub-cellular responses to UVA in relation to carcinogenesis. *International Journal of Radiation Biology,* 85**,** 177-195.

RYTER, S. W. & TYRRELL, R. M. 2000. The heme synthesis and degradation pathways: role in oxidant sensitivity: heme oxygenase has both pro-and antioxidant properties. *Free Radical Biology and Medicine,* 28**,** 289-309.

SKLAR, L. R., ALMUTAWA, F., LIM, H. W. & HAMZAVI, I. 2013. Effects of ultraviolet radiation, visible light, and infrared radiation on erythema and pigmentation: a review. *Photochemical & Photobiological Sciences,* 12**,** 54-64.

STEGE, H., BERNEBURG, M., HUMKE, S., KLAMMER, M., GREWE, M., GRETHER-BECK, S., BOEDEKER, R., DIEPGEN, T., DIERKS, K. & GOERZ, G. 1997. High-dose UVA1 radiation therapy for localized scleroderma. *Journal of the American Academy of Dermatology,* 36**,** 938-944.

TIAN, F., ZHANG, F., LAI, X., WANG, L., YANG, L., WANG, X., SINGH, G. & ZHONG, J. L. L. 2011. Nrf2-mediated protection against UVA radiation in human skin keratinocytes. *Bioscience trends,* 5**,** 23-29.

TYRRELL, R. M. 1996. Activation of mammalian gene expression by the UV component of sunlight–from models to reality. *Bioessays,* 18**,** 139-148.

TYRRELL, R. M. 2012. Modulation of gene expression by the oxidative stress generated in human skin cells by UVA radiation and the restoration of redox homeostasis. *Photochemical & Photobiological Sciences,* 11**,** 135-147.

VALENCIA, A. & KOCHEVAR, I. E. 2008. Nox1-based NADPH oxidase is the major source of UVA-induced reactive oxygen species in human keratinocytes. *J Invest Dermatol,* 128**,** 214-22.

WANG, M., SHI, G., BIAN, C., NISAR, M. F., GUO, Y., WU, Y., LI, W., HUANG, X., JIANG, X. & BARTSCH, J. W. 2018. UVA Irradiation Enhances Brusatol-Mediated Inhibition of Melanoma Growth by Downregulation of the Nrf2-Mediated Antioxidant Response. *Oxidative medicine and cellular longevity,* 2018.

WLASCHEK, M., HEINEN, G., POSWIG, A., SCHWARZ, A., KRIEG, T. & SCHARFFETTER-KOCHANEK, K. 1994. UVA-INDUCED AUTOCRINE STIMULATION OF FIBROBLAST-DERIVED COLLAGENASE/MMP-1 BY INTERRELATED LOOPS OFINTERLEUKIN–1 andINTERLEUKIN–6.*Photochemistry and photobiology,* 59**,** 550-556.

XIE, Y., JI, R. & HAN, M. 2019. Eriodictyol protects H9c2 cardiomyocytes against the injury induced by hypoxia/reoxygenation by improving the dysfunction of mitochondria. *Experimental and therapeutic medicine,* 17**,** 551-557.

YANG, S., ZHOU, B., XU, W., XUE, F., NISAR, M. F., BIAN, C., HUANG, X., YANG, L., ZHANG, Y. & BARTSCH, J. W. 2017. Nrf2-and Bach1 May Play a Role in the Modulation of Ultraviolet A-Induced Oxidative Stress by Acetyl-11-Keto-β-Boswellic Acid in Skin Keratinocytes. *Skin pharmacology and physiology,* 30**,** 13-23.

YORK, N. R. & JACOBE, H. T. 2010. UVA1 phototherapy: a review of mechanism and therapeutic application. *International journal of dermatology,* 49**,** 623-630.

ZHONG, J.-D., FENG, Y., LI, H.-M., XIA, X.-S. & LI, R.-T. 2016. A new flavonoid glycoside from Elsholtzia bodinieri. *Natural product research,* 30**,** 2278-2284.

ZHONG, J. L., EDWARDS, G. P., RAVAL, C., LI, H. & TYRRELL, R. M. 2010. The role of Nrf2 in ultraviolet A mediated heme oxygenase 1 induction in human skin fibroblasts. *Photochemical & Photobiological Sciences,* 9**,** 18-24.

ZHONG, J. L., RAVAL, C. M., NISAR, M. F., BIAN, C., ZHANG, J., YANG, L. & TYRRELL, R. M. 2014. Development of Refractoriness of HO-1 Induction to a Second Treatment with UVA Radiation and the Involvement of Nrf2 in Human Skin Fibroblasts. *Photochemistry and photobiology,* 90**,** 1340-1348.

ZHONG, J. L., YANG, L., LÜ, F., XIAO, H., XU, R., WANG, L., ZHU, F. & ZHANG, Y. 2011. UVA, UVB and UVC induce differential response signaling pathways converged on the eIF2α phosphorylation. *Photochemistry and photobiology,* 87**,** 1092-1104.

ZHOU, D., LEE, H. S., VILLARREAL, F., TENG, A., LU, E., REYNOLDS, S., QIN, C., SMITH, J. & SUNG, K. P. 2005. Differential MMP-2 activity of ligament cells under mechanical stretch injury: An in vitro study on human ACL and MCL fibroblasts. *Journal of Orthopaedic Research,* 23**,** 949-957.

ZUCKER, S. N., FINK, E. E., BAGATI, A., MANNAVA, S., BIANCHI-SMIRAGLIA, A., BOGNER, P. N., WAWRZYNIAK, J. A., FOLEY, C., LEONOVA, K. I. & GRIMM, M. J. 2014. Nrf2 amplifies oxidative stress via induction of Klf9. *Molecular cell,* 53**,** 916-928.